The Effect of Plastic Deformation on Low Temperature Mechanical and Magnetic Properties of Austenite 316LN Tube for ITER TF Conductor

Soo-Hyeon Park, Jun Young Kim, Won Woo Park, Heekyung Choi, Young Jae Ma, Soun Pil Kwon, Keeman Kim, Sung Chan Kang, and Dong Hee Lee

***Abstract*—While the manufacturing of superconducting CICC (cable in conduit conductor) and winding conductors into winding packs for ITER TF magnets, cold work is unavoidably applied on the jacketing tube. This article investigates the effect of plastic deformation on low temperature mechanical and magnetic properties of austenite 316LN stainless steel tube for ITER TF conductor. To simulate the manufacturing process of TF magnet, tubes were compacted, extended to 2.5% in longitudinal direction and heat treated. After each step, specimens were sectioned using wire cutting EDM, and tensile tests at 4 K, magnetic susceptibility measurements, and hardness tests have been carried out on those specimens. Remarkable reductions of elongation at failure have been observed as the amount of cold work is increased through compaction and extension. Further, correlations among results of tensile tests, magnetic susceptibility measurements and hardness tests are presented.**

***Index Terms*—Austenite stainless steel, cryogenics, magnetic susceptibility, plastic deformation, tensile test.**

I. Introduction

THE "round-in-round" jacket of the ITER TF conductor is made up of modified 316LN stainless steel tubes. One of the critical technical requirements is the low temperature (< 7 K) tensile test in which the elongation at failure shall be larger than 20 percent after the compaction, longitudinal extension, and the heat treatment of tubes which mimic processes for the fabrication of magnets [1], [2].

It is well known that the plastic deformation on austenite stainless steel via cold works such as drawing, rolling, etc. results strain hardening and reduction of the ductility [3]–[5]. Further, there are references which report the formation of the martensite phase due to the cold work [6], [7]. It is physically natural that uniaxial or biaxial deformation reduces the ductility and alters the lattice symmetry of material, which determines most of electronic, magnetic, and mechanical properties of metals combined with the chemical composition. However, up to our knowledge, there are no references which investigated the relation of low temperature mechanical and magnetic properties of this specific material (modified SS316LN) whose high Nickel contents make the Austenite phase very stable in the Schaeffler diagram.

We have carried out low temperature tensile tests, Vickers hardness tests, and cryogenic AC magnetic susceptibility measurements on four different kinds of specimens which undergone different amount of deformations and thermal cycle from a same virgin tube. Sample preparation, experimental procedures are described, and correlations between mechanical and magnetic properties as functions of deformations are presented.

TABLE I
Chemical Composition of Base Materials

Weight contents %				
C	Si	Mn	P	S
0.012	0.146	1.696	0.0175	0.0016
Cr	Ni	Mo	N	Co
17.271	13.550	2.555	0.1612	0.024

II. Experimental

A. Sample Preparation

Seamless stainless steel tubes are manufactured by hot extrusion of billets. Billets are machined from material which is produced by the electric arc furnace (EAF) steel making followed by the electro-slag-re-melting (ESR) process. Extruded tubes are cold drawn, solution annealed, straightened, and bright annealed for the final products. Specified length, outer diameter, and thickness of tubes are 13.0 m, 48.0 $\pm$ 0.2 mm, and 1.9 $\pm$ 0.1 mm respectively. Table I shows test results of the chemical composition of material after the EAF process, and it satisfies requirements specified in [1].

The ITER TF conductor is manufactured by insertion of a cable into the jacket which is assembled by butt welding of individual tubes, and compaction of the jacketed cable to the final dimension and spooling to a specified diameter ($\sim$4 m) are followed. Finally, in order to achieve the formation of A15 phase for the superconducting state of the cable, heat treatment at 650°C for 100 to 200 hours is needed. During these series

Manuscript received September 12, 2011; accepted November 11, 2011. Date of publication November 21, 2011; date of current version May 24, 2012. This work was supported by the Ministry of Education, Science and Technology of Korea and the Ministry of Knowledge Economy of Republic of Korea under a contract of the ITER Korea Project (2009-0081593).

S.-H. Park, W. W. Park, H. Choi, Y. J. Ma, S. P. Kwon, and K. Kim are with the National Fusion Research Institute, Daejeon 305-333, Korea (e-mail: shpark@nfri.re.kr).

J. Y. Kim is with the National Fusion Research Institute, Daejeon, 305-333, Korea, and also with the Department of Nuclear Fusion and Plasma Science, University of Science and Technology (UST), Daejeon, Korea.

S. C. Kang and D. H. Lee are with POSCO Specialty Steel, Shinchon-dong, Changwon, South Gyeongsang Province, Korea (e-mail: sungchan.kang@poscoss.com; dhlee1248@poscoss.com).

Color versions of one or more of the figures in this paper are available online at http://ieeexplore.ieee.org.

Digital Object Identifier 10.1109/TASC.2011.2176894

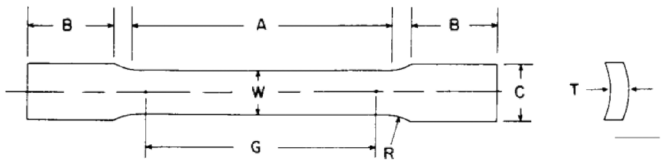

Fig. 1. Schematic of a specimen for the tensile test, conforming to ASTM E8M. The specific dimensions are provided in Table II.

TABLE II
SPECIMEN DIMENSIONS ACCORDING TO ASTM E8M

Parameter	*Dimension (mm)*
Gage length	50.0 ± 0.1
Reduced section width	12.5 ± 0.2
Specimen thickness	Tube wall thickness
Radius of fillet	≥ 12.5
Length of reduced section	≥ 60
Length of grip section	≥ 75
Width of grip section (approximate)	20

of operations, tubes undergo plastic deformations and thermal aging, and it is considered that there are four different states.

1) As Is (AI) state, in which tubes are in the initial state before compaction.
2) Compacted (CO) state, in which tubes are compacted to the diameter 43.7 mm [1], and thickness increases to 2.0 mm. Degree of plastic deformation is 5% in this process.
3) Compacted and Extended (COEX) state, in which additional cold work by spooling is applied.
4) Compacted, Extended, and Heat Treated (COEXHT) state.

To get each representative tube for above states, tube section whose length is 2 m was compacted by the Nippon Steel Engineering who is performing the jacketing of ITER TF Conductor for Japan. Spooling condition was incarnated through stretching 450 mm length compacted tube by 2.5% using a tensile machine. Stretched tube was heat treated at 650°C for 200 hours in a vacuum furnace which is evacuated with a cryopump, and the pressure remained at low 10^{-6} torr during the heat treatment. The ramp up rate was 25°C per hour.

Specimens for tensile tests were prepared from four different tubes conforming to ASTM E8M by electro discharge machining (EDM). Fig. 1 and Table II provide schematics and dimensions for the specimens consistent with ASTM E8M Fig. 13 specimen 1.

B. Low Temperature Tensile Tests

Tensile tests were performed using a commercial machine (MTS Alliance RT100) and a custom cryostat equipped with a liquid helium level meter, a clip-on extensometer whose gage length is 25 mm, and a calibrated cernox temperature sensor. Fig. 2 is a photograph of the insert in which a specimen is mounted for the test. The insert is immersed in liquid helium in the cryostat (which is not shown in the figure), and the level of helium and temperature are monitored during tests. Detailed procedures are described elsewhere [9].

Once liquid helium level is assured to be over the specimen grip set and temperature is lowered to the boiling point of liquid helium, test begins. Typical temperature during test was not 4.2 K, but 4.3 K because pressure of the cryostat is

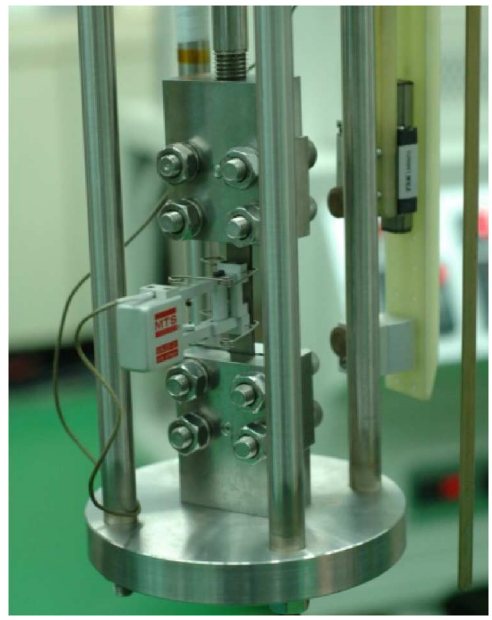

Fig. 2. The insert with specimen mounted. An extensometer is clipped on the specimen. Rightmost rod is the liquid helium level meter, and a cernox sensor is attached on the supporting rod with kapton tape (See yellow part whose location is above the specimen grip set).

slightly over than 1 bar. The crosshead moving rate is 0.5 ∼ 1.0 mm/min., which corresponds to $1.7 \sim 3.3 \times 10^{-4}$ sec^{-1} in the unit of strain rate, and that is well below than the rate recommended in [2]. With the given dimension of a specimen, stress was calculated from the load, strain was monitored by the extensometer reading. The elongation at break was determined by fitting broken pieces and measuring marked gage length.

C. Cryogenic AC Susceptibility Measurements

AC susceptibility is a frequency dependent property, which reflects the dynamics, i.e., time dependent phenomena of an electron spin or magnetic dipole system. It is a specific example of the linear response function [10] and defined as

$$M(t) = \int_{-\infty}^{t} \chi(t - t')H(t')dt' \tag{1}$$

where M is the magnetization, χ is the AC susceptibility, and H is the applied magnetic field. It is more convenient in a linear system to take the Fourier transform and write the relationship as a function of frequency. If we drive the magnetic field in the sinusoidal way, i.e., $H = H_0 \cos(\omega t)$, the integral becomes

$$M(\omega) = \chi(\omega)H(\omega) \tag{2}$$

It is a complex quantity which is composed of real and imaginary parts, due to the retarded response of the system to the time varying magnetic field.

AC susceptibility was measured at 4.0 K with a commercial magnetometer (PPMS AC Magnetization option). The frequency range was from 100 Hz to 10 kHz. The amplitude of the applied magnetic field was 10 Oe. Samples were cut by Electro Discharge Machining (EDM) from each tube, and typical dimension is 5 mm × 10 mm × 2 mm. To remove surface

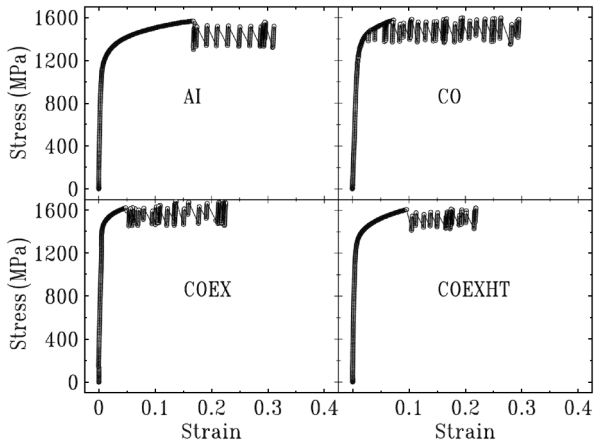

Fig. 3. Stress as a function of strain for four specimens. One can clearly see that elongation at break decreases as cold works are applied. For the meaning of abbreviations AI, CO, COEX, and COEXHT, see text.

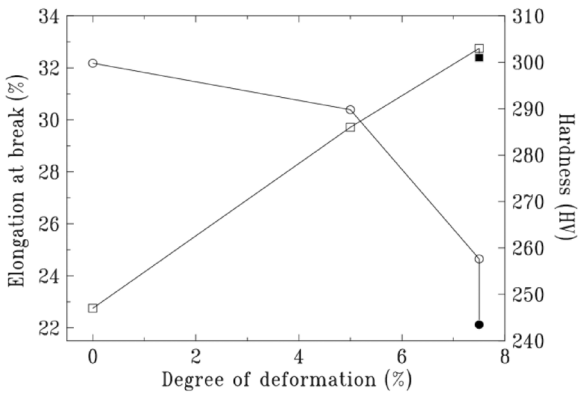

Fig. 4. Average elongation at break (circles) and Vickers hardness (squares) as functions of degree of deformation. Filled symbols represent data of heat treated samples. Lines are guides to the eye. As the deformation increases, the elongation decreases and hardness increases. Effect of heat treatment is not clear in the result of hardness.

oxides which influence magnetic susceptibility measurements, EDM cut surfaces were mechanically polished, cleaned and deoxidized by Hydrochloric acid.

D. Vickers Hardness Measurements

Vickers hardness measurements were done at room temperature by a commercial instrument (Mitutoyo HM-124) with same samples for the AC susceptibility measurements. Load and loading time was 0.5 kg and 10 sec respectively.

III. Results and Discussion

Fig. 3 shows stress as a function of the strain for four specimens from each different state of tubes. Data are displayed in the same scale intentionally, in order that one can assess the effect of the plastic deformations on the low temperature mechanical properties. All data show *Portevin-Le Chatelier effect (PLC)*, which represents serrated stress-strain curve shape that appears very often in cryogenic tensile tests. Two samples from each tube were tested and the elongations at break were averaged. Fig. 4 is a simultaneous plot of the average elongation and Vickers hardness as functions of degree of deformation. As mentioned in the first section, we also can observe reduction of the ductility and strain hardening as a result of the plastic deformation.

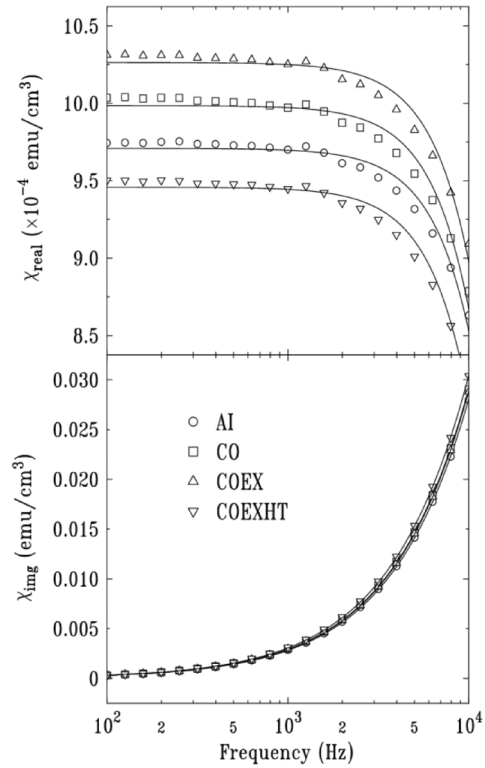

Fig. 5. Frequency dependence of real and imaginary parts of AC susceptibility. Different symbols represent four states of deformation. Lines are results of least square fit of experimental data to the Debye relaxation model (See text.).

One peculiar point is that whereas the heat treatment reduces ductility considerably, hardness is rarely affected. Hardness slightly decreases after the heat treatment, but the difference can be regarded within experimental error. We will address the effect of the heat treatment later again.

Fig. 5 shows the frequency dependence of real and imaginary parts of AC susceptibility at 4.0 K. To analyse the experimental data, we adopt the Debye relaxation model [11] in which complex $\chi(\omega)$ is expressed as follows.

$$\chi(\omega) = \chi_\infty + \frac{\Delta\chi}{1 + i\omega\tau} \tag{3}$$

where χ_∞ is the susceptibility at the high frequency limit, and $\Delta\chi = \chi_{static} - \chi_\infty$, where χ_{static} is the static, low frequency limit susceptibility, and τ is the characteristic relaxation time of the system. Separation into real and imaginary parts yields

$$\chi_{real}(\omega) = \chi_\infty + \Delta\chi \frac{1}{1 + \omega^2\tau^2} \tag{4}$$

$$\chi_{img}(\omega) = \Delta\chi \frac{\omega\tau}{1 + \omega^2\tau^2} \tag{5}$$

We have compared the experimental data to (4)–(5), and lines in Fig. 5 are results of simultaneous least square fit of real and imaginary parts. Most important properties what we can extract from the analysis are χ_{static} and τ, which represent the static and dynamic properties respectively. Deformation dependences of these two quantities are presented in Fig. 6.

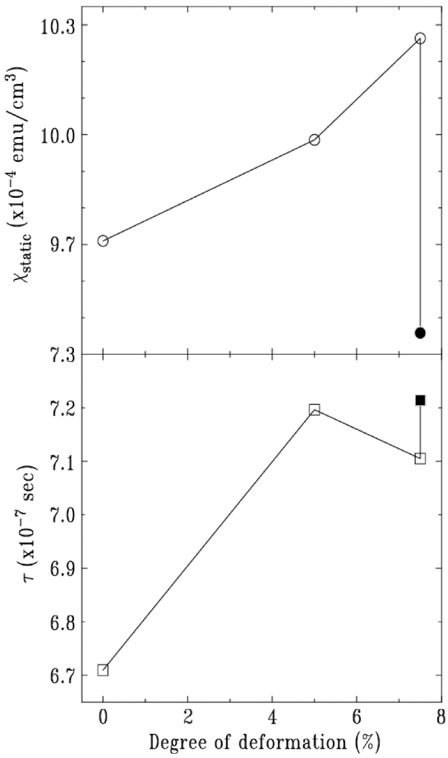

Fig. 6. Static susceptibility and relaxation time versus degree of deformation. Filled symbols represent data of heat treated sample. Lines are guides to the eye.

We can clearly observe that the static or DC magnetic susceptibility increases about 6% as the deformation increases. In other words, applying cold works on this Austenite stainless steel makes it *more magnetic*. At this stage, it is too premature to conclude that the amount of plastic deformation of this article ($\sim$7.5%) induces structural transformation into the martensite phase. It is also difficult to assess the amount of the martensite phase from the magnetic susceptibility measurements because there are no available magnetic data on the martensite phase which possibly formed through the deformation in this article. Systematic studies on the effect of larger deformation and the investigation of the lattice symmetry using x-ray or neutron diffraction will be helpful for the clarification of this matter.

To estimate the Austenitic stability, we have calculated Md_{30} temperature, which represents the lowest temperature where 50% of induced martensite is formed with a true strain of 0.3. One of the equations used to estimate the value is given as [11]

$$\mathrm{Md}_{30}(^{\circ}\mathrm{C}) = 551 - 462(\mathrm{C}+\mathrm{N}) - 9.2\mathrm{Si} - 8.1\mathrm{Mn} - 13.7\mathrm{Cr} - 29(\mathrm{Ni}+\mathrm{Cu}) - 18.5\mathrm{Mo} - 68\mathrm{Nb} - 1.42(\mathrm{d}-8) \quad (6)$$

where d is the ASTM grain size. Calculated Md_{30} with chemical composition in Table I is 91 K, which is much lower than room temperature at which deformation on samples is applied.

The effect of the heat treatment on the magnetic properties is not consistent in our data. Although the heat treatment reduces the ductility (See Fig. 4), magnetic susceptibility is reduced also, contrary to the expectation based on the above explanation. One of the possible explanations is that the heat treatment plays a role of reversion of the formed martensite phase.

Fig. 6 indicates that the relaxation time tends to increase as the deformation increases. However, it is hard to say that the system slows down as magnetic phase transition occurs [12], because experimental frequency window is so narrow and well below compared to the time scale ($\sim 10^{-7}$ sec) of the dynamics.

IV. Summary and Conclusion

Low temperature tensile test, Vickers hardness test, and cryogenic AC susceptibility measurements have been performed on four stainless steel tubes which have undergone different amount of plastic deformation and thermal cycle. Results strongly indicate that mechanical properties are in close relation with magnetic properties. Strain hardening and reduction of the ductility accompany growth of magnetic signal.

Effects of the heat treatment on mechanical and magnetic properties are not clearly understood with our data. Further study on this topic and precise refinement of crystal structure of deformed samples would be beneficial.

Acknowledgment

Soo-Hyeon Park thanks Dr. K. Wiess and Dr. K. Hamada for their efforts on cross-check of cryogenic tensile tests and valuable discussion on results.

References

[1] "Procurement arrangement 1.1.P6A.KO.01.0," Annex B, pp. 41–42.
[2] "Standardization of TF conductor jacket mechanical testing procedure," [Online]. Available: https://user.iter.org/?uid=33X9BT
[3] A. K. De, J. G. Speer, D. K. Matlock, D. C. Murdock, M. C. Mataya, and R. J. Comstock, "Deformation-induced phase transformation and strain hardening in type 304 austenitic stainless steel," *Metallurgical and Materials Trans. A*, vol. 37, no. 6, pp. 1875–1886, Jun. 2006.
[4] A. S. Domarevaa, A. A. Dobrikova, B. M. Efrosa, Ya. E. Beigelzimera, and V. N. Varyukhina, "Structure, hardening and failure of high nitrogen austenite steels after plastic deformation under pressure," *High Pressure Research*, vol. 15, no. 4, pp. 221–232, 1997.
[5] M. A. Filippov, R. A. Zil'bershtein, and V. E. Lugovykh, "Phase transformation and hardening of unstable austenitic steels in plastic deformation and impact action," *Metal Science and Heat Treatment*, vol. 23, no. 9, pp. 640–642, Sep. 1981.
[6] W. Ozgowicz, A. Kurc, and M. Kciuk, "Effect of deformation-induced martensite on the microstructure, mechanical properties and corrosion resistance of X5CrNi18-8 stainless steel," *Archives of Materials Science and Engineering*, vol. 43, no. 1, pp. 42–53, May 2010.
[7] D. F. Li, C. G. Fan, Y. Y. Li, and H. M. Cheng, "Tensile properties and deformation-induced martensitic transformation at cryogenic temperatures in Fe-Cr-Ni-Mn-N alloys," *Advances in Cryogenic Engineering (Mater)*, vol. 42, pp. 307–314, 1995.
[8] H. C. Kim, D. K. Oh, S.-H. Park, K. Kim, and P. Bruzzone, "Development and SULTAN test result of ITER conductor sample of Korea," *IEEE Trans. Appl. Supercond.*, vol. 18, pp. 1084–1087, 2008.
[9] R. Kubo, "Statistical-mechanical theory of irreversible processes. I. General theory and simple applications to magnetic and conduction problems," *J. Phys. Soc. Jpn.*, vol. 12, pp. 570–586, 1957.
[10] R. M. Hill and L. A. Dissado, "Debye and non-Debye relaxation," *J. Phys. C, Solid State Phys.*, vol. 18, no. 19, pp. 3829–3836, Jul. 1985.
[11] K. Nohara, Y. Ono, and N. Ohasi, *Trans. ISIJ*, vol. 17, p. 306, 1997.
[12] N. Goldenfeld, *Lectures on Phase Transitions and the Renormalization Group*. Reading, MA: Addison-Wesley, 1992, p. 133.